Bull. Chem. Soc. Jpn., **68**, 528—538(1995)

Simulation of the Valence X-Ray Photoelectron Spectra of 16 Polymers by the Semiempirical HAM/3 MO Method Using the Model Molecules

Kazunaka Endo,* Chiaki Inoue, Yasuo Kaneda, Masayuki Aida, Naoya Kobayashi, and Delano P. Chong*,†

Tsukuba Research Laboratory, Mitsubishi Paper Mills, Ltd., 46 Wadai Tsukuba, Ibaraki 300-42

†Department of Chemistry, University of British Columbia,
2036 Main Mall, Vancouver, B. C., Canada V6T 1Z1

(Received August 12, 1994)

The HAM/3 method was used to provide a better assignment of the valence X-ray photoelectron spectra of 16 polymers involving nitrogen, oxygen, fluorine, a glucose unit, and a benzene nucleus using the monomer, dimer or trimer model molecules without consideration of the contraction factor of the energy scale. The calculated Al $K\alpha$ photoelectron spectra were obtained using Gaussian functions of a fixed approximate linewidth, 0.10 I_k and $I_k = I'_k - WD$, where I'_k is the vertical ionization potential of each MO and WD is an approximate shift to account for the work function of the sample and other energy (polarization energy and so on) effects. We assumed that WD corresponds to the shift that we must apply before we can compare the calculated spectrum for the single model molecule with the observed spectrum for the solid. The approximate linewidth corresponds to the experimental result that the inner valence spectra are broader. The theoretical spectra showed good agreement with the spectra of the polymers observed between 0—40 eV.

Recent studies[1—13] have shown that information on polymer structures can be obtained from ultraviolet-ray photoelectron spectra (UPS) and X-ray photoelectron spectra (XPS) when interpreted with MO calculations on simple model oligomers. To analyze the photoelectron spectra of polymers, we need to estimate the wavefunction of the cationic state corresponding to each MO losing an electron after X-ray irradiation. However, we can simulate the XPS using Koopmans' theorem and the usual MO calculations of the ground state for N electrons using ab initio and semiempirical MO methods. In previous studies,[11—13] we used shifts of about 10 eV on Koopmans' values to analyze the valence XPS of polymers using MO calculations by the HONDO and PM3 programs.[14,15]

As is often the case in the framework of the MO techniques, the calculations of the ground-state yield very wide valence electronic structures and the contractions of the energy scale become necessary to obtain the best fit between the theoretical energy levels and the experimental XPS peak positions. The contraction factors, then, vary with the system under study. For example, the values of 0.77 and 0.82 for valence effective hamiltonian (VEH)[16,17] and STO-3G basis[6] ab initio investigations, respectively, have been used in comparisons made between the calculated and the experimental valence spectra. Thus, for a better assignment of the valence XPS of polymers in nitrogen, oxygen, and fluorine, we tested the performance of the semiempirical MO method called hydrogenic atoms in molecule, version 3 (HAM/3).[18—20] This MO method does not need a contraction, because it uses the idea of "transition states"[21] rather than Koopmans' theorem to predict the vertical ionization potentials (VIPs) for the photoelectron spectra.[19]

For simulating the valence XPS using MO methods, the linewidth of the peak shape represented by a Gaussian or a Gaussian–Lorentian function was generally used as instrumental resolution values (e. g. 0.5, 0.7 eV and so on). Here, we used the Gaussian functions of an approximate linewidth (0.10 I_k),[22] implying that the spectra of the inner valence levels are broader.

In a previous study,[22] a new approach was tested by comparing the valence XPS of six polymers [$(-CH_2-CHR-)_n$ (R = H, CH_3, OH, and F), $(-CH_2-CH_2-NH-)_n$, and $(-CH_2-CH_2-O-)_n$] with HAM/3 results on the model n-mer molecules ($n = 2$ to 5). The results suggested that the trimer model is quite adequate in simulating valence XPS of solid polymers, when we introduced a shift WD to account for a sum of the work function and other energy effects. Consequently, the trimer model was used to study ten more polymers.[23] By now, we have simulated valence XPS of 60 polymers by this MO method. Here, we

used the monomer, dimer or trimer model molecules for 16 polymers (poly(vinylidene fluoride) (PVDF), poly(tetrafluoroethylene) (PTFE), poly(trifluoro vinyl acetate) (PVTFA), poly(4-vinylpyridine) (P4VP), poly(2-ethyl-2-oxazoline) (PEOX), nylon 6(N6), polyurethane (PU), polyurea (PUA), cellulose (CEL), ethylcellulose (ECEL), poly-4-hydroxystyrene (PHS), poly(2,6-dimethyl-1,4-phenylene oxide) (PDMPO), poly(oxyphenyleneoxyphenylenecarbonylphenylene) (PEEK), poly(styrene-co-maleic anhydride) (PSCMA), poly(ethylene terephthalate) (PET) and poly(bisphenol A carbonate) (PBAC)) to analyze the X-ray photoelectron spectra of the polymers by the HAM/3 method. The simulation was obtained by taking the VIP for each MO from the HAM/3 calculation and using the Gelius model[24] for molecular photoionization cross-section (PICS). The theoretical spectra were constructed from a superposition of the peaks centered at the calculated VIPs. The peak shape was represented by a Gaussian function.

Theoretical Background

When one uses the diffuse ionization model[19] in the HAM/3 method, the eigenvalues give the VIPs directly.

Because calculations for single molecules based on the trimer model are compared to experiments on a solid, we must shift each computed VIP I'_k by a quantity WD[25] as I_k $(E_F)=I'_k-WD$. This quantity (WD) denotes the sum of the work function of the sample and other energy effects, such as the polarization energy, the width of the interchain band formation and the peak broadening in the solid state.[2,3,26—29] In this work, approximate values of WD ranging from 4 to 5 eV were chosen to the nearest 0.5 eV by inspection to provide the best agreement on the location of the main features of the simulated spectrum.

The successful trimer model was used for many of the polymers (PVDF, PTFE, PVTFA, P4VP, PEOX, PHS) in the present study. For other polymers, we tested the model dimers and monomers. In those cases, the number of atoms in the model n-mer is at least 35. It should be noted that the model monomer is not the same as the monomer. For simplicity, consider teflon (PTFE) as an example (although we actually used the model trimer for it). The monomer is CF_2=CF_2, while the model monomer is CF_3–CF_3. Thus, the model molecules [H–$(CH_2$–$CF_2)_3$–H, F–$(CF_2$–$CF_2)_3$–F, H–$(CH_2$–CH–$(OCOCF_3))_3$–H, H–$(CH_2$–CH(C_5H_4N) (4-vinylpyridine))$_3$–H, H–$((C_2H_5)$C–O–CH_2–CH_2–N(2-ethyl-2-oxazoline))$_3$–H, H–$((CH_2)_5$–CO–NH$)_2$–H, H–(CO–NH–C_6H_4–CH_2–C_6H_4–NH–CO–O–$(CH_2)_4$–O)–H, H–(CO–NH–C_6H_4–CH_2–C_6H_4–NH–CO–NH–$(CH_2)_3$–NH)–H, H–$(C_6H_{10}O_5)_2$–H, H–$(C_{12}H_{22}O_5)$–H, H–$(CH_2$–CH–$(C_6H_4OH))_3$–H, H–$(C_6H_3(CH_3)_2$–O$)_2$–H, H–(C_6H_4–O–C_6H_4–O–C_6H_4–CO)–H, H–$(CH_2$–CH(C_6H_5)–CH–(COO)–CHCO))$_2$–H, H–(O–CO–C_6H_4–CO–O–$(CH_2)_2)_2$–H, H–(C_6H_4–C$(CH_3)_2$–C_6H_4–O–CO–O)–H] were calculated by the semiempirical HAM/3 program (the new version extended by Chong).[30] For the geometry of the molecules, we used the optimized structures from the semi-empirical AM1 (version 6.0) method.[15] In the HAM/3 and AM1 programs, we enlarged the maximum number of occupied MOs and atoms as 300 and 75, respectively, to calculate the model molecules.

In the HAM/3 program, we can obtain the semiempirical relative PICS of the Gelius model,[24] and the ab initio relative PICS for both Mg $K\alpha$ (1253.6 eV) and Al $K\alpha$ (1486.6 eV) radiation of Nefedov et al.[31] based on the Hartree–Fock–Slater methods. The atomic PICS, as described by Nefedov, was obtained under the assumption that the electrostatic atomic field was spherically symmetrical. In the present study, we used the relative PICS values for each AO in Table 1.

In order to simulate the valence XPS of polymers theoretically, we constructed from a superposition of peaks centered on the VIPs, I_k. The peak shape is represented by a Gaussian function,

$$f(x) = A(k) \exp\{-B(k)(x - I_k)^2\}, \quad (1)$$

where the intensity (A(k)) is estimated from the relative PICS for Al $K\alpha$ radiation. For B(k), we use the linewidth $WH(k)=2(Ln^2/B(k))^{1/2}$. The linewidth is introduced for two reasons: (a) we are approximating the density of states by discrete MO levels, and (b) each state has a natural line width due to instrumental resolution, electronic relaxation processes, vibrational broadening and so on. By trial and error, we found that simulated spectra have a reasonable appearance when we choose a simple form for the linewidth as WH(k)=0.10 I_k for monomer, dimer, or trimer molecule.

Experimental

The experimental photoelectron spectra of 16 polymers were obtained on a Perkin–Elmer model PHI 5400 MC ESCA spectrometer, using monochromatized Al $K\alpha$ radiation. The spectrometer was operated at 600 W, 15 kV, and 40 mA. The photon energy was 1486.6 eV. A pass energy of 35.75 eV was employed for high-resolution scans in a va-

Table 1. Relative Photoionization Cross-Section (PICS) of Each Atomic Orbital for H, C, N, O, and F Atoms (Relative to C2s)

Atomic	Orbital	Al $K\alpha$ (Nefedov et al.[31])
H	1s	0.0093
C	2s	1.0000
	2p	0.0324
N	2s	1.8210
	2p	0.0902
O	2s	2.9480
	2p	0.2029
F	2s	4.4290
	2p	0.4016

Table 2. Observed Peaks, VIP, Main AO PICS, Orbital Nature, and Functional Group for Valence XPS of PVDF [(The Gap between Observed and Calculated VIPs)=4.0 eV]

Peak (eV)	VIP (eV)	Main AO PICS	Orbital nature[b)]	Functional group
33.0	38.66;38.25;37.97	F2s	sσ(F2s–C2s)–B,	F–C
(28—40)[a)]	36.34;36.00;35.94	F2s	pσ (F2s–C2p)–B	F–C
20.5	25.48;24.10;22.43	C2s(0.8), F2s(0.2)	sσ(C2s–C, F2s)–B	–C(main chain), C–F
(18—24)[a)]				
16.0	20.85;19.79;19.60	C2s(0.4), F2s, F2p	{pσ(C2s–F, C2p)–B,	C–F, –C(main chain)
(14.5—18)[a)]			sσ(C2s–F2s)–B}	C–F
13.0	{17.87;17.85;17.48;	F2p, C2p, F2s	{pσ(C2p–F2s)–B,	C–F, –C(main chain)
(11.5—14.5)[a)]	17.25;17.22}		$p\pi_p$(F2p, C2p–C2p)–B}	
	(16.10—16.86)	F2p, C2p, F2s, C2s	{ $p\pi_p$(F2p, C2p–C2p)–B,	C–F, –C(main chain)
			pσ(C2p–C2s)–B}	
9.5	(13.05—13.99)	F2p	pπ (lone pair)–NB	F–C
(5—11.5)[a)]	Below 15.09 eV			
	many adjacent levels			
	15.09;14.77;14.22	F2p	$p\pi_p$(F2p, C2p–C2p)–B	C–F
	12.15;11.61;10.97	F2p, C2p	pπ (lone pair)–NB	F–C

a) Shows the peak range. b) π_p indicates the pseudo π orbitals of the C–F. B and NB mean bonding and nonbonding, respectively. (C, F2s–2p) means (C2s–C2p) and (F2s–F2p), (C2p, F2p–C2p) denotes (C2p–C2p) and (F2p–C2p), and so on.

Table 3. Observed Peaks, VIP, Main AO PICS, Orbital Nature, and Functional Group for Valence XPS of PTFE [(The Gap between Observed and Calculated VIPs)=4.0 eV]

Peak (eV)	VIP (eV)	Main AO PICS	Orbital nature[b)]	Functional group
35.5	41.63—38.78	F2s	sσ(F2s–C2s)–B,	F–C
(28—40)[a)]	38.65—37.93	F2s	pσ (F2s–C2p)–B	F–C
21.5	26.71;25.56;24.13	C2s(0.7), F2s(0.3)	sσ(C2s–C, F2s)–B	–C(main chain), C–F
(20—25)[a)]				
16.0	20.43—19.03	F2s, F2p, C2s	{pσ(F2p–C2s)–B,	F–C
(14—20)[a)]			pσ(C2p–F2s)–B}	
	22.79;21.93;21.82	F2s, F2p, C2s	{pσ(F2p–C2s)–B,	F–C
			pσ(C2p–F2s)–B}	
11.5	Below 17.66 eV	F2p	{pπ(lone pair)–NB,	F–C
(8—14)[a)]	Many adjacent levels		$p\pi_p$(F2p, C2p)–B}	

a) Shows the peak range. b) π_p indicates the pseudo π orbitals of the C–F. B and NB mean bonding and nonbonding, respectively. (C, F2s–2p) means (C2s–C2p) and (F2s–F2p), (C2p, F2p–C2p) denotes (C2p–C2p) and (F2p–C2p), and so on.

Table 4. Observed Peaks, VIP, Main AO PICS, Orbital Nature, and Functional Group for Valence XPS of PVTFA [(The Gap between Observed and Calculated VIPs)=4.0 eV]

Peak (eV)	VIP (eV)	Main AO PICS	Orbital nature[b)]	Functional group
33.0	39.87;39.64;39.62	F2s	sσ(F2s–C2s)–B,	F_3C–
(30—40)[a)]	{36.88;36.84;36.67;	F2s	pσ (F2s–C2p)–B	F_3C–
	36.63;36.60;36.57}			
28.0	33.44;33.10;33.08	O2s	sσ(O2s–C2s)–B	–O–C, C=O
(22—30)[a)]	31.93;31.58;31.49	O2s	pσ(O2s–C2p)–B	C=O, –O–C
18.0	{25.29;23.98;23.04;	C2s(0.7), O2s, F2p	s, pσ(C2s–O2s, F2p)–B	–C–C–C, O–C–C–F
(16.5—22)[a)]	22.67;22.45;21.85}	F2s(0.4), C2s, F2p	s, pσ(C2s–F2s, 2p)–B	C–F
14.0	18.14—18.52	F2s(0.5), F2p	pσ(F2s–C2p)–B	F–C
(12—16.5)[a)]	18.72—20.48	C2s, F2p, O2p	pσ(C2s–F, O2p)–B	C–F, C–O, C=O
	16.78—17.56	O2p, C2s	pσ(C2s–O2p)–B	C–O, C=O
10.0	13.13—14.80	F2p(0.8), O2p, C2p	$p\pi_p$(F, O2p–C2p)–B,	O–C–C–F
(7—12)[a)]	Many adjacent levels			
	15.00—16.18	O2p, O2s, C2s	pπ, pσ(O2p—C2p, 2s)–B	–O–C, O=C
	12.02—13.03	O2p, C2p	$p\pi_p$, π(O2p–C2p)–B	–O–C, C=O
5.5	11.73;11.48;11.04	O2p	pπ(lone pair)–NB	–O–C, C=O
(4—7)[a)]	10.63;10.36;10.34	O2p	pπ(lone pair)–NB	C=O, –O–C

a) Shows the peak range. b) π_p indicates the pseudo π orbitals of the C–F. B and NB mean bonding and nonbonding, respectively. (C, F2s–2p) means (C2s–C2p) and (F2s–F2p), (C2p, F2p–C2p) denotes (C2p–C2p) and (F2p–C2p), and so on.

Table 5. Observed Peaks, VIP, Main AO PICS, Orbital Nature, and Functional Group for Valence XPS of P4VP [(The Gap between Observed and Calculated VIPs)=5.0 eV]

Peak (eV)	VIP (eV)	Main AO PICS	Orbital nature[b)]	Functional group
22.5	28.06;27.94;27.86	N2s(0.6), C2s(0.4)	sσ(N2s–C2s)–B,	–C–N=C–(pyridine)
(21—26)[a)]				
18.0	21.70—22.95	C2s(0.8), N2s	sσ (C2s–2s)–B	–C=C–(pyridine)
(16—21)[a)]	23.28—26.13	C2s(0.6), N2s(0.2)	sσ(C2s–N2s)–B	{–C–(main chain); =C–N=C–(pyridine)}
15.0	18.82;18.72;18.69	C2s(0.6), N2p	pσ(C2s–N, C2p)–B	–C=C–N=(pyridine)
(12—16)[a)]	19.29—20.16	C2s	sσ(C2s–C2s)–B	–C–(main chain)
	17.50—17.84	C2s(0.6), N2s, C2p	sσ, pσ(C2s, 2p–N2s)–B	=C–N=C–(pyridine)
10.5	15.44—16.03	C2s, N2s, C2p	pσ(C2p–C2s, N2s)–B	{=C–N=C–(pyridine),
(6—12)[a)]	Many adjacent levels			–C–(main chain)}
	13.54—15.36	C2p, N2p	pπ, pπ$_p$(C, N2p–C2p)–B	=C–N=C–, –C–
	11.41—12.91	N2p, C2p	pπ, pπ$_p$(N, N2p–C2p)–B	=C–N=C–, –C–
4.5	8.90;8.77;8.70	N2p, C2p	pπ(N, C2p–C2p)–B	=C–N=C–(piridine)
(3—6)[a)]	9.11—9.92	C2p, N2p	pπ(C, N2p–C2p)–B	=C–N=C–(piridine)

a) Shows the peak range. b) B and NB mean bonding and nonbonding, respectively. (C, N2s–2p) means (C2s–C2p) and (N2s–N2p), (C2p, N2p–C2p) denotes (C2p–C2p) and (N2p–C2p), and so on.

Table 6. Observed Peaks, VIP, Main AO PICS, Orbital Nature, and Functional Group for Valence XPS of PEOX [(The Gap between Observed and Calculated VIPs)=5.0 eV]

Peak (eV)	VIP (eV)	Main AO PICS	Orbital nature[b)]	Functional group
26.5	31.17;30.59;30.28	O2s(0.8), N2s, C2s	sσ(O, N2s–C2s)–B	C–O–C, C–N–C
(25—30)[a)]				
23.5	28.55;27.93;27.31	{N2s(0.5), O2s(0.4),	sσ (N, O2s–C2s)–B,	C–O–C, C–N–C
(21—25)[a)]		C2s(0.1)}	pσ(N, O2s–C2p)–B	C–O–C, C–N–C
18.5	{24.34;24.19;23.90;	C2s	sσ(C2s–2s)–B	–C–C–
(17—21)[a)]	22.68;22.64;22.31}	C2s(0.7), O2s, N2s	sσ(C2s–O, N2s)–B	C–O–C, C–N–C
15.5	18.65—21.14	{C2s(0.5), O2s,	{pσ(C2s–N2p)–B,	–C–N–C–
(14—17)[a)]		N2p, C2p}	pσ(C, O2s–C2p)–B}	–C–C, C–O–C
(6—14)[a)]	11.29—17.61	O2p, N2p, C2p	pσ(O, N, C2p–C2p)–B	C–O–C, C–N–C
	Many adjacent levels		pπ$_p$(O, C, N2p–C2p)–B	C–O–C, C–N–C
4.0	10.27;9.99	O2p, N2p	pπ(lone pair)–NB	–O–, –N–
(2.5—5)[a)]	8.63—9.44	N2p, O2p	pπ(lone pair)–NB	–N–, –O–

a) Shows the peak range. b) π_p indicates the pseudo π orbitals of the C–O, C–N, C–C bonds. B and NB mean bonding and nonbonding, respectively. (C, N2s–2p) means (C2s–C2p) and (N2s–N2p), (C2p, N2p–C2p) denotes (C2p–C2p) and (N2p–C2p), and so on.

Table 7. Observed Peaks, VIP, Main AO PICS, Orbital Nature, and Functional Group for Valence XPS of N6 [(The Gap between Observed and Calculated VIPs)=5.0 eV]

Peak (eV)	VIP (eV)	Main AO PICS	Orbital nature[b)]	Functional group
26.5	30.66;30.37	O2s(0.7), N2s, C2s	{sσ(O2s–C2s)–B,	–C=O
(24.5—30)[a)]			pσ(O2s–C2p)–B}	
23.0	28.24;27.32	N2s(0.6), O2s(0.4)	pσ (N, O2s–C2p)–B	–N–C, O=C
(21—24.5)[a)]				
19.0	22.79—24.79	C2s	sσ(C2s–2s)–B	–C–C–
(16—21)[a)]	21.41;20.67	C2s	sσ(C2s–2s)–B	–C–
14.0	18.06—19.59	C2s(0.7), N2p, O2s	pσ(C2s–N2p)–B	–C–N
(12—16)[a)]				
10.5	10.87—16.96	O2p, N2p, C2p	{pπ(O, N, C2p–C2p)–B,	C=O, –C–N
(5—12)[a)]	Many adjacent levels		pσ(C2p–H1s)–B}	$-CH_2$
3.5	9.07;8.91;8.74;8.60	O2p, N2p	pπ(lone pair)–NB	O=C, C–N
(3—5)[a)]				

a) Shows the peak range. b) B and NB mean bonding and nonbonding, respectively. (C, N2s–2p) means (C2s–C2p) and (N2s–N2p), (C2p, N2p–C2p) denotes (C2p–C2p) and (N2p–C2p), and so on.

Table 8. Observed Peaks, VIP, Main AO PICS, Orbital Nature, and Functional Group for Valence XPS of PU [(The Gap between Observed and Calculated VIPs)=4.0 eV]

Peak (eV)	VIP (eV)	Main AO PICS	Orbital nature[b)]	Functional group
26.0	{31.87;31.82;29.93	O2s(0.8), C2s, N2s	{sσ(O, N2s–C2s)–B,	–O–C, O=C, –N–C
(21—32)[a)]	29.86;29.83	O2s	pσ (O2s–C2p)–B}	O=C, –O–C
	28.70;28.58	N2s(0.6), O2s, C2s	pσ (N, O2s–C2p)–B	–N–C, O=C, –O–C
	26.38;25.60	C2s(0.7), N2s, O2s	sσ(C2s–C, N2s)–B	–C–, C=C–, –C–N–
17.5	22.41;22.39;22.05	C2s	sσ(C2s–C2s)–B	–C–, C=C–
(15—21)[a)]	23.93;23.42	C2s	sσ(C2s–2s)–B	–C–, C=C–
	19.54—21.36	C2s(0.8)	pσ(C2s–O, N2p)–B	–C–, –C–N–, –C–O
13.5	18.04;17.81	C2s(0.5), N2p, O2p	pσ(C2s–N, O2p)–B	–C–, –C–N–, C–O
(12—15)[a)]	18.51;18.78	C2s(0.4), O2s, N2p	pσ(C2s–N, C2p)–B	–C–, –C–N–, C–O
	17.57;17.70	C2s(0.5), N2p, C2p	pσ(C2s–N, C2p)–B	–C–, –C–N–
10.0	13.53;13.48	O2s(0.6), O2p, C2p	pσ(O2p–O2s, C2p)–B	O=C
(7—11)[a)]	Many adjacent levels			
	13.62—16.53	O2p, N2p, C2p	pσ(O, N, C2p–C2p)–B	–C–, –C=, N–C–O, C=O
	12.29—13.22	O2p, N2p, C2p	pπ, π_p(O, C, N2p–C2p)–B	–C=C–, C=O, N–C–O
5.5	9.20—11.35	O2p, N2p	pπ(lone pair)–NB	C–N–
(2.5—7)[a)]	Many adjacent levels			
	11.41—11.97	C2p	pπ(C2p–C2p)–B	–C=C–
	8.10—8.90	O2p, N2p, C2p	pπ(lone pair)–NB	O=, –O–, –N–, –C=

a) Shows the peak range. b) B and NB mean bonding and nonbonding, respectively. (C, N2s–2p) means (C2s–C2p) and (N2s–N2p), (C2p, N2p–C2p) denotes (C2p–C2p) and (N2p–C2p), and so on.

Table 9. Observed Peaks, VIP, Main AO PICS, Orbital Nature, and Functional Group for Valence XPS of CEL [(The Gap between Observed and Calculated VIPs)=5.0 eV]

Peak (eV)	VIP (eV)	Main AO PICS	Orbital nature[b)]	Functional group
26.0	30.52—32.39	O2s	sσ(O2s–C2s)–B	–O –C–
(22—32)[a)]	29.85—30.31	O2s	sσ, pσ(O2s–C2s, C2p)–B	–O–C–
18.0	{24.71;24.15;	C2s(0.7), O2s	sσ(C2s–C2s, O2s)–B	C–C–, C–O–
(17—21)[a)]	23.33;23.12}	C2s(0.9), O2s	sσ(C2s–C2s, O2s)–B	C–C–, C–O–
14.0	17.97—19.99	C2s(0.6), O2p	sσ, pσ(C2s–C2s, 2p, O2p)–B	C–C–, C–O–
(12—17)[a)]	21.42;21.03;20.58	C2s(0.8), O2s	sσ(C2s–C, O2s)–B	C–C–, C–O
7.0	10.75—12.98	O2p(0.6), C2p	pπ(O, C2p–O, C2p)–B	–O–C–, C–C
(3—12)[a)]	Many adjacent levels			
	13.17—16.82	O2p(0.5), C2p	pπ(C2p, O2p–C2p)–B	–O–C–, C–C
	9.20—10.13	O2P	pπ(lone pair)–NB	–O–

a) Shows the peak range. b) B and NB mean bonding and nonbonding, respectively. (C, O2s–2p) means (C2s–C2p) and (O2s–O2p), (C2p, O2p–C2p) denotes (C2p–C2p) and (O2p–C2p), and so on.

Table 10. Observed Peaks, VIP, Main AO PICS, Orbital Nature, and Functional Group for Valence XPS of PHS [(The Gap between Observed and Calculated VIPs)=4.5 eV]

Peak (eV)	VIP (eV)	Main AO PICS	Orbital nature[b)]	Functional group
27.5	30.96;30.91;30.88	O2s	{sσ(O2s–C2s)–B,	–O–C–
(24—31)[a)]			pσ(O2s–C2p)–B}	
20.5	24.74—26.68	C2s	sσ(C2s–C2s)–B	–C–C–, –C=C–(benz)
(19—24)[a)]				
17.5	21.09—23.87	C2s	sσ(C2s–C2s)–B	–C=C–(benz), –C–C–
(16—19)[a)]				
14.5	18.22—19.58	C2s	sσ(C2s–C2s)–B	–C=C–(benz), –C–C–
(11.5—16)[a)]	16.12—17.43	C2s(0.7), O2p	pσ, sσ(C2s–O2p, C2s)–B	–C–O, –C=C–(benz)
10.0	13.20—14.14	C2p, O2p	pπ(C2p–C, O2p)–B	–C=C–(benz), C–O–
(5—11.5)[a)]	Many adjacent levels			
	14.22—15.64	C2p, C2s	pπ, pσ(C2p–C2p, 2s)–B	–C=C–(benz), –C–C–
	10.44—12.94	O2p, C2p	pπ(O, C2p–C2p)–B	–O–C, –C=C–(benz), –C–C–
4.5	8.19—9.07	O2p, C2p	{pπ(lone-pair)–NB,	–O–
(2—5)[a)]			pπ(C2p–C2p)–B}	–C=C–(benz)

a) Shows the peak range. b) B and NB mean bonding and nonbonding, respectively. (C, O2s–2p) means (C2s–C2p) and (O2s–O2p), (C2p, O2p–C2p) denotes (C2p–C2p) and (O2p–C2p), and so on. (benz) means benzene nucleus.

Table 11. Observed Peaks, VIP, Main AO PICS, Orbital Nature, and Functional Group for Valence XPS of PEEK [(The Gap between Observed and Calculated VIPs)=5.0 eV]

Peak (eV)	VIP (eV)	Main AO PICS	Orbital nature[b)]	Functional group
27.0	31.50;31.10;30.50	O2s(0.9), C2s	{sσ(O2s–C2s)–B,	–O–C–, O=C
(23—31)[a)]			pσ(O2s–C2p)–B}	
20.5	26.50;26.01;25.48	C2s(0.8), O2s	sσ(C2s–C, O2s)–B	{–C=C–(benz),
(19—23)[a)]				C–O–, C=O}
17.5	21.43—23.13	C2s(0.9), O2s	sσ(C2s–C2s)–B	{–C=C–(benz),
(16—19)[a)]				C–O–, C=O}
14.0	17.29—18.65	C2s(0.6), O2p	pσ, sσ(C2s–O2p, C2s)–B	{–C=C–(benz), –C–O–
(11.5—16)[a)]	16.01—16.62	O2p, C2p, C2s	{pσ(C2s–O2p, C2s)–B,	–C–O, –C=C–(benz)
			pπ(C2p–C, O2p)–B}	
9.5	13.02—15.21	C2p, O2p, C2s	{pπ(C2p–C, O2p)–B,	{C–O–, C=O,
(5—11.5)[a)]	Many adjacent levels		pσ(C2p–C2s)–B}	–C=C–(benz)}
	10.52—12.70	O2p, C2p	pπ(O, C2p–C2p)–B	–O–C, –C=C–(benz), –C=O
3.5	8.12—9.49	O2p, C2p	{pπ(lone-pair)–NB,	–O–, =O
(2—5)[a)]			pπ(C2p–C2p)–B}	–C=C–(benz)

a) Shows the peak range. b) B and NB mean bonding and nonbonding, respectively. (C, O2s–2p) means (C2s–C2p) and (O2s–O2p), (C2p, O2p–C2p) denotes (C2p–C2p) and (O2p–C2p), and so on. (benz) means benzene nucleus.

Table 12. Observed Peaks, VIP, Main AO PICS, Orbital Nature, and Functional Group for Valence XPS of PSCMA [(The Gap between Observed and Calculated VIPs)=5.0 eV]

Peak (eV)	VIP (eV)	Main AO PICS	Orbital nature[b)]	Functional group
28.0	31.86—33.07	O2s(0.9), C2s	sσ, pσ(O2s–C2s, 2p)–B	–O–C, O=C
(23—32)[a)]	30.53 ; 30.37	O2s	pσ, sσ(O2s–C2p, 2s)–B	O=C, –O–C
20.0	25.28—27.16	C2s	sσ(C2s–C2s)–B	{–C=C–(benz),
(19—22)[a)]				–C–C(main cahin)}
17.0	20.41—24.07	C2s	sσ(C2s–C2s)–B	{–C=C–(benz),
(15—19)[a)]				–C–C(main cahin)}
13.5	17.20—19.74	C2s(0.6), O2s, O2p	pσ, sσ(C2s–O2p, O, C2s)–B	{–C=C–(benz), –C–O–,
(12—15)[a)]				–C–C(main cahin), C=O}
11.0	13.44—15.16	O2p, O2s, C2s, C2p	{pπ(O, C2p–C2p)–B,	{O=C, –C=C–(benz)
(7—12)[a)]	Many adjacent levels		pσ(C2p–C, O2s)–B}	–C–C, –C–O–}
	15.41—16.14	O2p, C2s, C2p	pπ, pσ(O, C2p–C2p, 2s)–B	–C=C–(benz), O=C, –O–C
	11.30—13.36	O2p, C2p	pπ(O, C2p–C2p)–B	O=C, –C=C–(benz)
6.0	9.84—11.05	O2p	{pπ(O2p–C2p, lone-pair}–B, NB	O=C, –O–
(2—7)[a)]	9.01—9.37	C2p	pπ(C2p–C2p)–B}	–C=C–(benz)

a) Shows the peak range. b) B and NB mean bonding and nonbonding, respectively. (C, O2s–2p) means (C2s–C2p) and (O2s–O2p), (C2p, O2p–C2p) denotes (C2p–C2p) and (O2p–C2p), and so on. (benz) means benzene nucleus.

Table 13. Observed Peaks, VIP, Main AO PICS, Orbital Nature, and Functional Group for Valence XPS of PET [(The Gap between Observed and Calculated VIPs)=4.0 eV]

Peak (eV)	VIP (eV)	Main AO PICS	Orbital nature[b)]	Functional group
27.0	31.28;32.04;31.95	O2s(0.9), C2s	sσ(O2s–C2s)–B	–O–C–, O=C
(23—32)[a)]	29.44;30.37	O2s	pσ(O2s–C2p)–B	O=C, –O–C
18.5	21.25;23.82	C2s	sσ(C2s–C2s)–B	–C=C–(benz), –C–C–
(16—22)[a)]	25.66—26.87	C2s(0.8), O2s	sσ(C2s–C, O2s)–B	–C=C–(benz), O=C–O–
14.0	17.12—19.96	C2s(0.5), O2p	sσ, pσ(O2s–C2s, O2p)–B	–C=C–(benz), O=C–O–
(12—16)[a)]	15.60—16.84	O2p, C2p, C2s	pπ, pσ(O, C2p–C2p, C2s)–B	O=C–O, –C=C–(benz)
11.0	14.09—14.86	O2p, C2p, O2s	{pπ(O, C2p–C2p)–B,	O=C–O, –C=C–(benz)
(6—12)[a)]	Many adjacent levels		pσ(C2p–O2s)–B}	O=C–O
	11.66—13.79	O2p, C2p	pπ(O, C2p–C2p)–B	O=C–O, –C=C–(benz)
5.0	9.12—10.65	O2p, C2p	pπ(O, C2p–C2p, lone pair)–B,NB	O=C–O, –C=C–(benz)
(3—6)[a)]	7.44—7.88	O2p, C2p	pπ(O2p–C2p)–B	O=C–O

a) Shows the peak range. b) B and NB mean bonding and nonbonding, respectively. (C, O2s–2p) means (C2s–C2p) and (O2s–O2p), (C2p, O2p–C2p) denotes (C2p–C2p) and (O2p–C2p), and so on. (benz) means benzene nucleus.

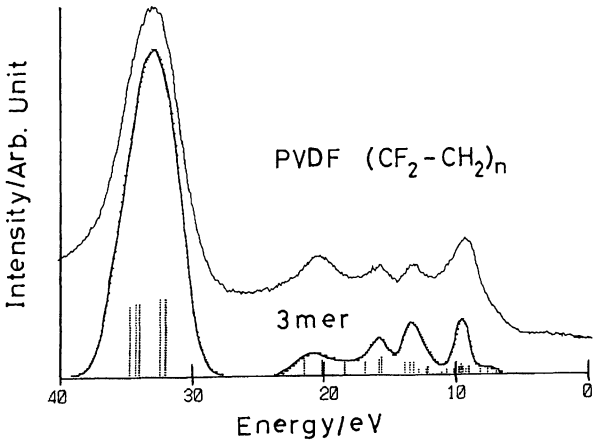

Fig. 1. Valence XPS of PVDF with the simulated spectra and with the spectral patterns of the trimer model molecules as calculated using HAM/3.

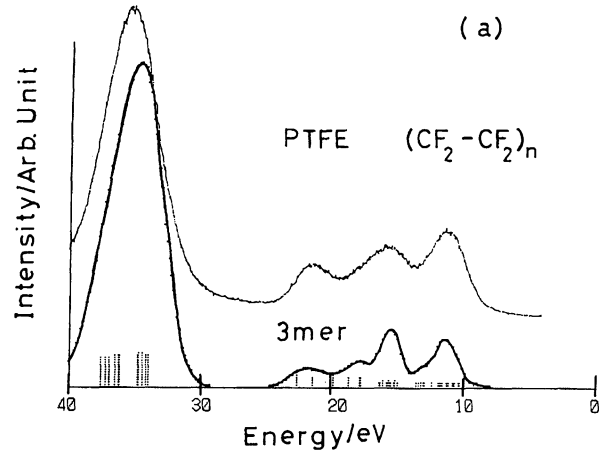

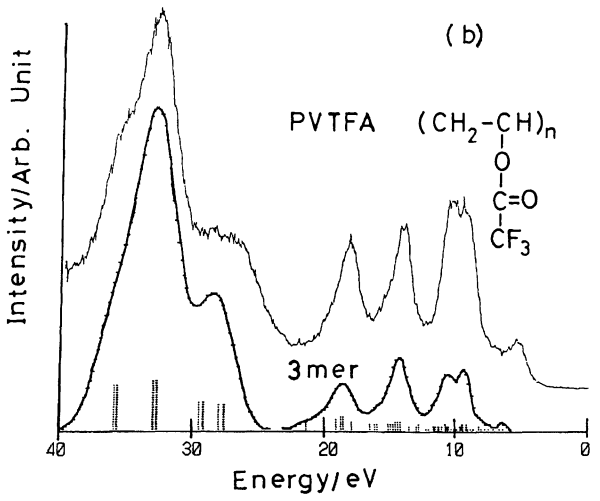

Fig. 2. (a) and (b). Valence XPS of PTFE and PVTFA, respectively, with the simulated spectra and with the spectral patterns of the trimer model molecules as caluclated using HAM/3.

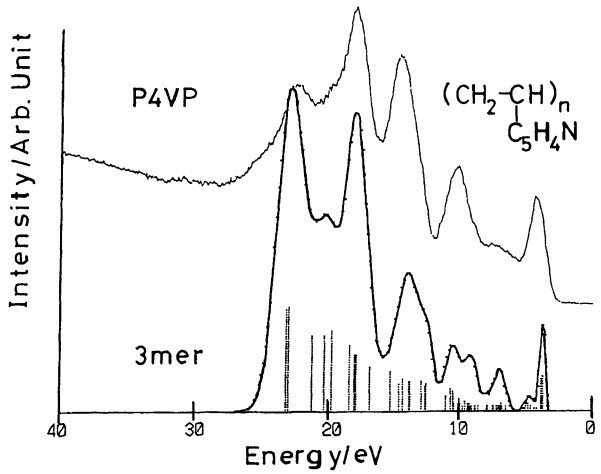

Fig. 3. Valence XPS of P4VP with the simulated spectra and with the spectral patterns of the trimer model molecules using HAM/3.

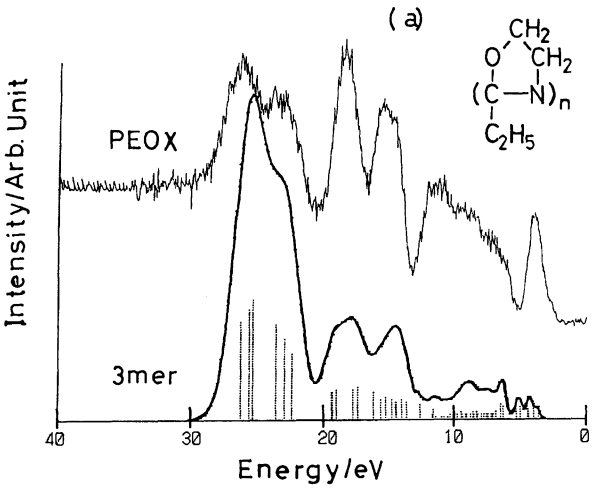

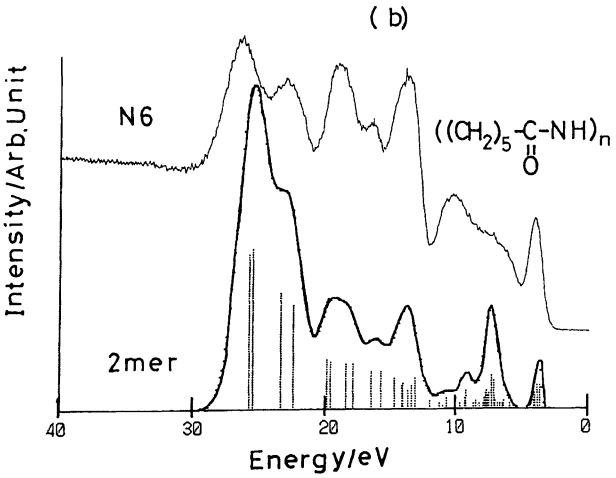

Fig. 4. (a) and (b). Valence XPS of PEOX and N6 with the simulated spectra and with the spectral patterns of the trimer and dimer model molecules, respectivley, as caluclated using HAM/3.

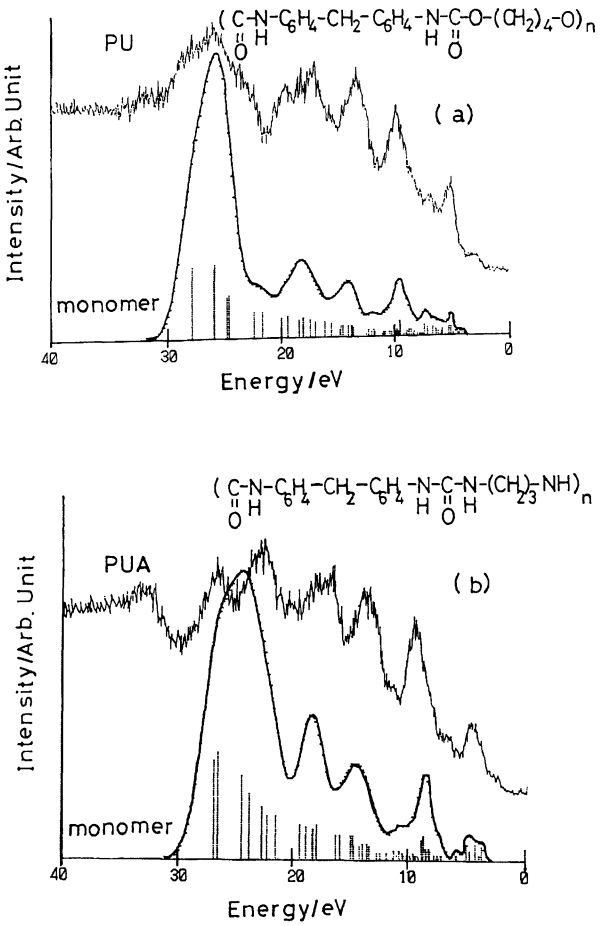

Fig. 5. (a) and (b). Valence XPS of PU and PUA, respectively, with the simulated spectra and with the spectral patterns of the monomer model molecules using HAM/3.

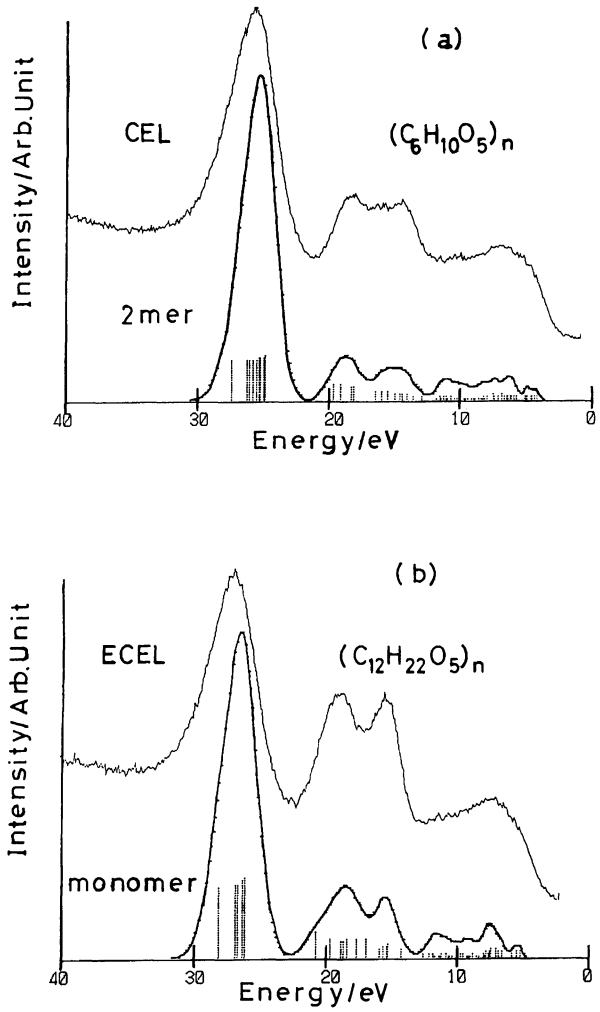

Fig. 6. (a) and (b). Valence XPS of CEL and ECEL, respectively, with the simulated spectra and with the spectral patterns of the dimer and monomer model molecules using HAM/3.

lence binding energy analysis (50 eV of range). The angle between the X-ray source and the analyzer was fixed at 45°. The spot size in the measurement was 3×1 mm.

The use of dispersion compensation yielded an instrumental resolution of 0.5 eV with the full width at half-maximum on the Ag3d line of silver. Multiple-scan averaging on a multi channel analyzer was used for the valence binding energy region, although a very low photoelectron emission cross section was observed in this range.

We used commercially-available poly(vinylidene fluoride) (PVDF) (Aldrich Chemical Co., Inc.; M_w 534000), poly(tetrafluoroethylene) (PTFE) (Scientific Polymer Products, Inc.), poly(trifluoro vinyl acetate) (PVTFA) (Scientific Polymer Products, Inc.), poly(4-vinylpyridine) (P4VP) (Scientific Polymer Products, Inc.), poly(2-ethyl-2-oxazoline) (PEOX) (Aldrich Chemical Co., Inc.; M_w 200000), nylon 6 (N6) (Aldrich Chemical Co., Inc.), cellulose (CEL) (Scientific Polymer Products, Inc.; M_w 64800—81000), ethylcellulose (ECEL) (Hercules, Inc. N200), poly-4-hydroxystyrene (PHS) (Scientific Polymer Products, Inc.), poly(styrene-co-maleic anhydride) (PSCMA) (Scientific Polymer Products, Inc.; M_w 50000), poly(oxyphenyleneoxyphenylenecarbonylphenylene) (PEEK) (ICI Chemical Co., Inc.), poly(2,6-dimethyl-1,4-phenylene oxide) (PDMPO) (Aldrich Chemical Co., Inc.; M_w 244000), poly(ethylene terephthalate) (PET) (ICI Chemical Co., Inc.) and poly(bisphenol A carbonate) (PBAC) (Aldrich Chemical Co., Inc.; M_w 64000). For PVDF, PTFE, PEEK, PDMPO, and PET, we used the film or the pressed disc. Other samples, except for PVTFA, were prepared by cast-coating the polymer solution on an aluminium plate, while water, methanol, ethanol, chloroform, HFIP, THF, dioxane, and acetone were used for the CEL, P4VP, ECEL, PEOX, N6, PBAC, PHS, and PSCMA polymers, respectively. For PVTFA, the sample were prepared by derivatization of polyvinyl alcohol film on Al plate with trifluoroacetic anhydride. A low-energy electron flood gun was used in order to avoid any charging effect on the surface of the sample. The C1s line positions of the CH_2, CF_2, and C_6H_4 (or phenyl) groups on the polymer films or discs were used as calibration references of (285.0; 286.5), (292.5), and (284.5; 285.0) eV for (PVTFA, P4VP, N6, PEOX; PVDF, CEL, ECEL), (PTFE) and (PEEK, PET, PBAC; PHS, PDMPO, PSCMA), respectively.

For polyurethane(PU) and polyurea(PUA), we cited the valence XPS spectra by Beamson and Briggs.[32]

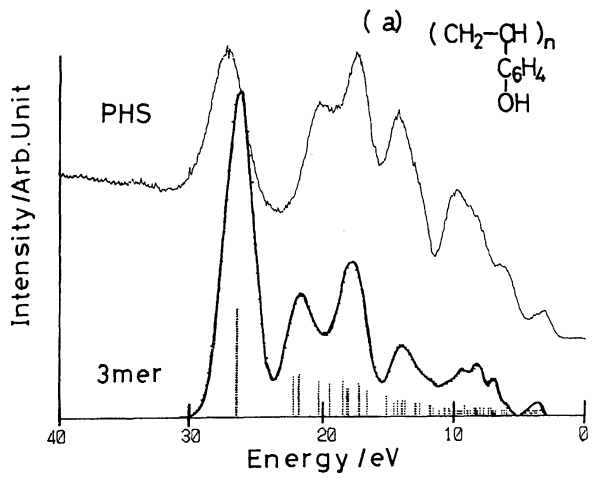

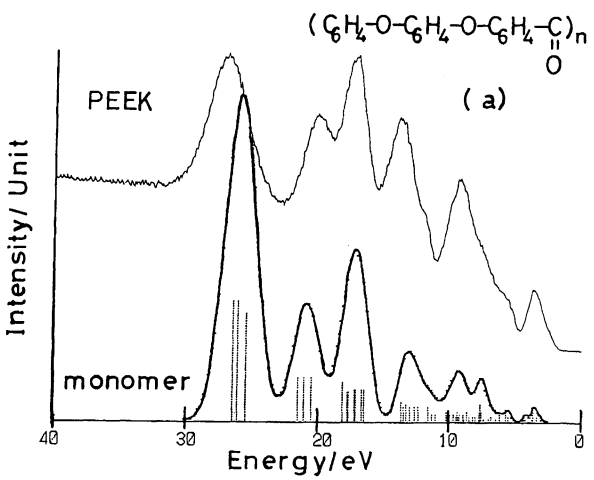

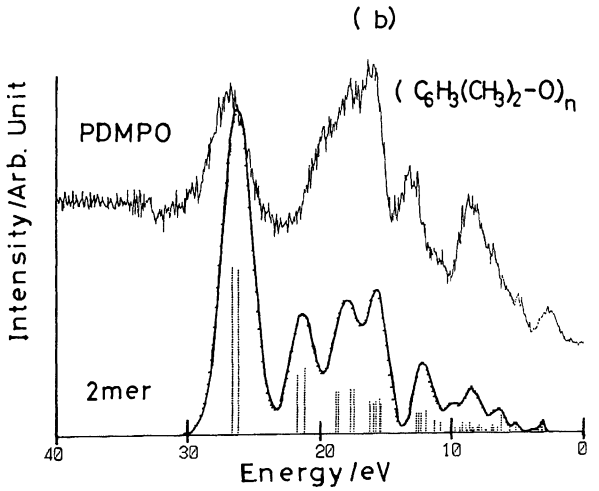

Fig. 7. (a) and (b). Valence XPS of PHS and PDMPO with the simulated spectra and with the spectral patterns of the trimer and dimer model molecules, respectively, using HAM/3.

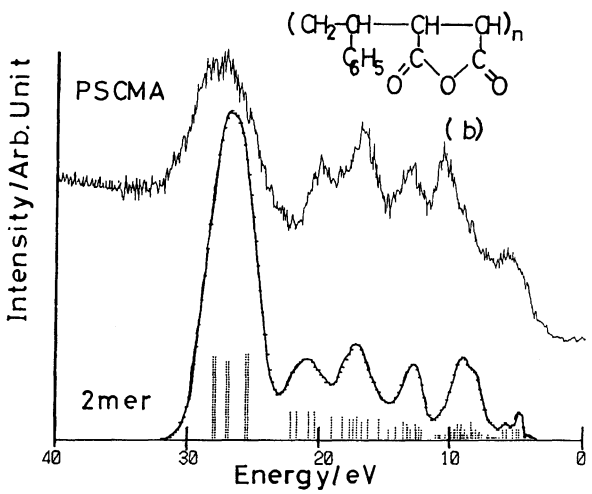

Fig. 8. (a) and (b). Valence XPS of PEEK and PSCMA with the simulated spectra and with the spectral patterns of the monomer and dimer model molecules, respectively, using HAM/3.

Results and Discussion

Vertical ionization potentials predicted by Koopmans' theorem are often too high, by approximately 8%. In contrast, the VIPs calculated by the HAM/3 method have an average absolute deviation of about 0.4 eV.[30,33] Moreover, wrong assignment of peaks in photoelectron spectra by the HAM/3 method is extremely rare. Based on such performance, we have some confidence in the modeling polymers by applying the HAM/3 method on the monomer, dimer or trimer model. The agreement between simulated and observed XPS of polymers gives us further assurance about our interpretation of the different regions of the spectra in this and other related studies.

(a) Valence XPS of 3 Polymers Involving Fluorine. In Figs. 1 and 2 (a,b), the simulated spectra of PVDF, PTFE, and PVTFA with the spectral patterns are compared with the observed XPS. As mentioned earlier, the simulation used a Gaussian lineshape function for each MO with a model linewidth of 0.10 I_k and $I_k = I'_k - \mathrm{WD}$. The simulated spectra using the trimer model are in very good accordance with the observed spectra of the polymers. The shift due to the WD effects was estimated as 4.0 for PVDF, PTFE, and PVTFA, respectively.

Tables 2, 3, and 4 show the observed peaks, the VIPs, the main AO PICS, the orbital nature and the functional group for PVDF, PTFE, and PVTFA, respectively. The intense spectra in the range of 30—40 eV (Figs. 1 and 2 (a,b) and Tables 2, 3, and 4), characteristic of F2s contributions, correspond to the VIP of $s\sigma$ (F2s–C2s)- and $p\sigma$ (F2s–C2p)-bonding orbitals. For PVTFA, the shoulder peak between 25 and 30 eV is due to the $s\sigma$ (O2s–C2s) and $p\sigma$ (O2s–C2p)-bondings of the side chain –O– and O=C groups. In these figures, the peaks at around 20 eV correspond to the VIP of $s\sigma$ (C2s–C2s)-bonding orbitals which result from the main

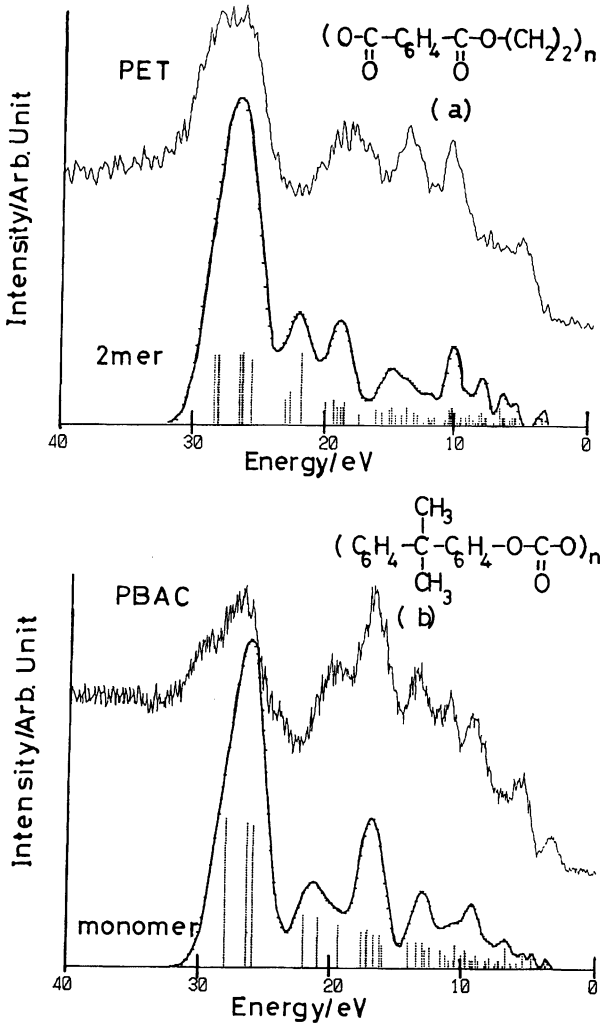

Fig. 9. (a) and (b). Valence XPS of PET and PBAC with the simulated spectra and with the spectral patterns of the dimer and monomer model molecules, respectively, using HAM/3.

chain –C–C– group.

(b) Valence XPS of 5 Polymers Involving Nitrogen. For P4VP (Fig. 3), intense spectra in the range of 20—25 eV are determined by N2s main contributions, while large peaks between 20 and 30 eV for PEOX, N6, PU, and PUA (Figs. 4 and 5) are due to both N2s and O2s main contributions, respectively. In these spectra, the double peaks between 12 and 20 eV result mainly from pσ (C2s–N2p) and sσ (C2s–C2s) bonding orbitals. The peaks (at around 5 eV) are due to lone-pair orbitals of main chain N and/or O for these polymers. We showed the orbital characters of P4VP, PEOX, N6, and PU in Tables 5, 6, 7, and 8. The shift due to work function effects was estimated as 5.0, 5.0, and 4.0 eV for (P4VP and PEOX), N6, and (PU and PUA), respectively. For these molecules also, the spectra appeared to show good agreement with the observed ones when we used an approximate linewidth of 0.10 I_k for monomer, dimer and trimer.

(c) Valence XPS of 8 Polymers Involving Glucose Unit, and Benzene Nucleus and Oxygen. For the eight polymers (Figs. 6, 7, 8, and 9), the theoretical spectra with the spectral patterns show good accordance with the experimental valence binding energy spectra. The differences of the fingerprint spectra between functional groups of the monomer unit for each polymer seem to be reflected in both the observed and simulated spectra. The shift due to WD effects was obtained as 4.0, 4.5, and 5.0 eV for (ECEL, PET), PHS, and (CEL, PDMPO, PEEK, PSCMA, and PBAC) polymers, respectively.

In Figs. 6, 7, and 8, the intense spectrum, which is due to O2s-dominant contribution at around 27 eV, corresponds to the theoretical values of sσ (O2s–C2s)-bonding and pσ (O2s–C2p)-bonding orbitals. In this assignment of the polymers which have both –O– and >C=O groups, for PEEK, PSCMA, PET, and PBAC, the sσ and pσ orbitals depend on the two components, –O– and >C=O. Tables 9, 10, 11, 12, and 13 show the orbital characters of the spectra for CEL, PHS, PEEK, PSCMA, and PET (similar tables for ECEL, PDMPO, and PBAC are omitted).

It is very interesting that we can observe the characteristic spectra which are due to the PICS for any atomic orbital of the constituent elements of the functional groups. For these 16 polymers, we have clarified the orbital nature of the fingerprint spectra which were characterized from the constituent elements (F, C, N, and O), in the range of 0—30 eV.

(d) Spectral Linewidths of Valence XPS for Polymers. As mentioned in a previous paper,[11] the spectral linewidths below 12 eV are determined by the broadening due to many adjacent MO energy levels. In contrast, the linewidths in the range of 13—40 eV may be governed by the relaxation of the inner valence 2s electron states for the MO levels. In this section, since the linewidths of F2s, N2s, or O2s spectra of the polymers were obtained as 2.5—4.0 eV, we describe the reason of the broadening.

The broadening of the inner-valence binding energy is partly due to the same reason as for gas-phase single molecules: The breakdown of the one-particle picture accompanying shake-up phenomena. The foot and the wing of the broader peak of the inner valence ionization result from transitions considered as mixing between single ionization and simultaneous ionization–excitation (shake-up) configurations.[30,35—38]

In another previous paper,[22] we proposed the meaning of the Gaussian functions of an approximate linewidth (0.10 I_k). This corresponds to the experimental result that the linewidth of spectra in the inner valence energy levels is broader than in the outer energy levels. In this study, the linewidth of 2s spectra (2.5—4 eV) was also broader than that of the 2p spectra. Let us assume that the linewidth being larger than the instrumental resolution of 0.5 eV can also be partly caused by

lifetime effects, and consider why the hole in the inner valence region has a shorter lifetime than that in the outer valence region. The hole of the 2s-orbital levels of polymers involving second-row atoms by X-ray radiation will be filled by electrons from the outer many adjacent occupied p-orbital levels through ultraviolet-ray emission process; the hole of the 2p-orbital levels is far from being filled by electrons, since there are no occupied levels above the 2p-orbital levels. Thus, the lifetime of the 2s-hole will be shorter than that of 2p-hole. Our approximate linewidth suggests the experimental results in the range of the valence band, 0—50 eV. A good fit between our simulation and the observed spectra of polymers seems to confirm that our general interpretation (discussed above) is reasonable.

References

1) C. B. Duke and A. Paton, in "Conductive Polymers," ed by B. Seymour, Plenum, New York (1981), p. 155.
2) K. Seki, in "Optical Techniques to Characterize Polymer Systems," ed by H. Baessler, Elsevior, Amsterdam (1989), p. 115.
3) C. H. Xian, K. Seki, H. Inokuchi, S. Hashimoto, N. Ueno, and K. Sugita, *Bull. Chem. Soc. Jpn.*, **58**, 890 (1985).
4) J. J. Pireaux, S. Svensson, E. Basilier, P. A. Malmqvist, U. Gelius, R. Caudano, and K. Siegbahn, *Phys. Rev. A*, **A14**, 2133 (1976).
5) J. J. Pireaux and R. Caudano, *Phys. Rev. B*, **B15**, 2242 (1977).
6) P. Boulanger, C. Magermans, J. J. Verbist, J. Delhalle, and D. S. Urch, *Macromolecules*, **24**, 2757 (1991).
7) P. Boulanger, R. Lazzaroni, J. J. Verbist, and J. Delhalle, *Chem. Phys. Lett.*, **129**, 275 (1986).
8) S. R. Cain, *Chem. Phys. Lett.*, **143**, 361 (1988).
9) P. Boulanger, J. Riga, J. J. Verbist, and J. Delhalle, *Macromolecules*, **22**, 173 (1989).
10) J. Delhalle, S. Delhalle, and J. Riga, *J. Chem. Soc., Faraday Trans. 2*, **1987**, 503.
11) K. Endo, N. Kobayashi, M. Aida, and C. Inoue, *J. Phys. Chem. Solids*, **54**, 887 (1993).
12) K. Endo, C. Inoue, N. Kobayashi, T. Higashioji, and H. Nakatuji, *Bull. Chem. Soc. Jpn.*, **66**, 3241 (1993).
13) K. Endo, C. Inoue, N. Kobayashi, and M. Aida, *J. Phys. Chem. Solids*, **55**, 471 (1994).
14) M. S. Dupuis, J. D. Watts, H. G. Villar, and G. J. B. Hurst, "HONDO, Version 7," Scientific and Engineering Computations Dept. 48B, IBM Corp., New York (1978), p. 12401.
15) J. J. P. Stewart, *J. Comput. Chem.*, **10**, 289 (1989).
16) E. Orti and J. L. Bredas, *J. Chem. Phys.*, **89**, 1009 (1988).
17) J. L. Bredas and T. C. Clarke, *J. Chem. Phys.*, **86**, 253 (1987); *Chem. Phys. Lett.*, **164**, 240 (1989) etc.
18) L. Åsbrink, C. Fridh, and E. Lindholm, *Chem. Phys. Lett.*, **52**, 63 (1977); *Quantum Chem. Program Exch.*, **12**, 398 (1980).
19) L. Åsbrink, C. Fridh, and E. Lindholm, *Chem. Phys. Lett.*, **52**, 69 (1977).
20) E. Lindholm and L. Åsbrink, "Molecular Orbitals and Their Energies, Studied by the Semiempirical HAM Method," Springer-Verlag, Berlin (1985).
21) J. C. Slater, *Adv. Quantum Chem.*, **6**, 1 (1972).
22) K. Endo, Y. Kaneda, M. Aida, and D. P. Chong, to be published.
23) M. Aida, Y. Kaneda, N. Kobayashi, K. Endo, and D. P. Chong, *Bull. Chem. Soc. Jpn.*, **67**, 2972 (1994).
24) U. Gelius and K. Siegbahn, *Faraday Discuss. Chem. Soc.*, **54**, 257 (1972); U. Gelius, *J. Electron Spectrosc. Relat. Phenom.*, **5**, 985 (1974).
25) J. Delhalle, J. M. Andre, S. Delhalle, J. J. Pireaux, R. caudano, and J. J. Vervist, *J. Chem. Phys.*, **60**, 595 (1974).
26) L. E. Lyons, *J. Chem. Soc.*, **1957**, 5001.
27) J. J. Pireaux and R. Caudano, *Phys. Rev. B*, **B15**, 2242 (1977).
28) C. B. Duke, in "Photon, Electron and Ion Probes of Polymer Structure and Properties," ACS Symp. Ser., Washington (1981), Vol. 162, p. 113.
29) W. R. Salanech, in "Photon, Electron, and Ion Probes of Polymer Structure and Properties," ACS Symp. Ser., Washington (1981), Vol. 162, p. 121 (1981).
30) D. P. Chong, *Can. J. Chem.*, **63**, 2007 (1985).
31) V. I. Nefedov, N. P. Sergushin, I. M. Band, and M. B. Trzhaskovskaya, *J. Electron Spectrosc. Relat. Phenom.*, **2**, 383 (1973).
32) G. Beamson and D. Briggs, "High Resolution XPS of Organic Polymers, the Scienta ESCA300 Database," John Wiley and Sons, New York (1992).
33) D. P. Chong, *Theor. Chim. Acta*, **51**, 55 (1979).
34) D. P. Chong, *Can. J. Chem.*, **61**, 1 (1983).
35) J. Duffy and D. P. Chong, *Org. Mass Spectrom.*, **28**, 321 (1993).
36) H. Nakatsuji and T. Yonezawa, *Chem. Phys. Lett.*, **87**, 462 (1982).
37) H. Nakatsuji, *Chem. Phys.*, **75**, 425 (1983).
38) H. Nakatsuji, *Chem. Phys.*, **76**, 283 (1983).